Numerical analysis of crack resistance and reinforcement stresses in hybrid steel-GFRP reinforced concrete beams

Ravshanbek Mavlonov [a)], Kamoliddin Muminov, Abdurasul Martazaev, Sohiba Numanova, Odiljon Fozilov

Namangan State Technical University, Namangan, Uzbekistan

[a)] *Corresponding author: ravshanbek.mavlonov@gmail.com*

Abstract. In this article, the reinforcement and concrete stresses, as well as the crack resistance of six types of hybrid steel-GFRP reinforced concrete beams and three types of conventional steel reinforced concrete beams, were investigated using ANSYS Workbench with the finite element method. A total of nine beams were studied in the numerical modeling, and the performance of hybrid steel–GFRP beams was compared to that of conventional steel reinforced concrete beams. The obtained results show that the steel reinforcement in the tension zone exceeded the yield stress, which allowed it to remain ductile and provided additional safety after yielding. Although cracks started earlier in the hybrid beams due to the lower stiffness of GFRP bars, their overall load-carrying capacity was not significantly lower than that of conventional reinforced concrete beams.

INTRODUCTION

For many years, steel has been utilized as the main material in construction for concrete structures, providing high strength and ductility. But its disadvantages cannot be disregarded. Steel reinforcement is prone to corrosion and concrete structures with steel rebar often require costly strengthening and repair, which affects durability. Furthermore, the building industry's environmental impact is further increased by the substantial CO_2 emissions linked to steel manufacturing [1-3]. Conventional methods of protecting steel bars from corrosion require highly complexity and cost. As a result, many countries are actively implementing different types of FRP reinforcements. Given current economic and environmental conditions, special attention has recently been given to the use of modern FRP reinforcements, especially glass fiber reinforced polymer (GFRP) bars, as a promising alternative to such issues [4, 5].

Compared to steel reinforcement, GFRP bars are up to four times lighter, non-conductive, non-magnetic, completely resistant to corrosion, and made from natural, eco-friendly and cost-effective raw materials. Nevertheless, since the lower modulus of elasticity of FRP bars relative to steel, they cannot fully replace steel rebar in load-bearing concrete structures [6]. Instead, effective work can be achieved by using hybrid reinforcement, where steel and GFRP bars are combined in the tension zone of concrete. Consequently, hybrid steel-FRP reinforced concrete beams represent an important innovative solution for ensuring structural strength, crack resistance, stiffness, and economic efficiency [7].

Corrosion of steel reinforcement in reinforced concrete structures significantly decreases structural safety and limits long-term exploitation. Although concrete gives a highly alkaline environment and forms a passive protective film on the surface of the rebar, which protects the steel from corrosion, the alkalinity of concrete decreases over time due to the carbonation process. As a result, in the presence of oxygen, moisture, and various aggressive chemical agents, corrosion of the reinforcement begins [8, 9]. However, corrosion does not occur simultaneously across all reinforcement bars. It usually occurs in zones near the outer surface, especially at the corners of the structure, which are the most affected. This happens due to a high carbonation, easy access of oxygen and moisture, and the increased susceptibility of corner concrete to deterioration. The deterioration of the concrete cover near the exterior surface accelerates the corrosion of the inner reinforcement as well [10-12].

The growing demand to strengthen and restore reinforced concrete structures can cause construction costs to rise

and encouraged the search for alternative engineering solutions. Traditional methods of preventing steel corrosion such as using corrosion resistant materials, resin coatings, cathodic protection, chemical admixtures, or concrete surface treatment have not been adopted, primarily due to their high costs or practical limitations [13].

Over the past years, FRP reinforcement is well known as a potential replacement for steel in the reinforcement and strengthening of concrete and reinforced concrete structures due to its higher tensile strength compared to steel and its resistance to corrosion. However, composite reinforcement exhibits a linearly elastic stress–strain behavior, which increases the risk of brittle failure when used in concrete members [14]. According to ACI 440.1R-06, the design of concrete beams reinforced with composite bars focuses on increasing ductility by utilizing the plastic deformation capacity of concrete in the compression zone, rather than relying on the rupture strain of the composite reinforcement. Moreover, the modulus of elasticity of GFRP bars is approximately four times lower than that of steel and about twice as high as that of conventional concrete [15]. Therefore, beams reinforced with GFRP bars have been found to exhibit lower crack resistance and reduced stiffness compared to reinforced concrete beams of the same size and with similar amounts of steel reinforcement [16].

As a result, the design guidelines require a reinforcement ratio greater than the balanced reinforcement ratio to ensure failure occurs due to concrete crushing in the compression zone rather than FRP bars rupture. This requirement usually leads to higher construction costs due to the relatively expensive FRP reinforcement. At this stage, completely replacing steel reinforcement with FRP bars does not seem a feasible option in elements where crack width and deflection control are important [17].

However, the application of hybrid steel-FRP reinforcement in concrete beams enables the expansion of the practical use of FRP bars. In this technique, FRP reinforcement is placed closer to the tensile zone of the beam due to its corrosion resistance, while steel reinforcement is arranged deeper inside with a larger concrete cover for the steel bars [18]. Using a combination of FRP and steel reinforcement in the tensile zone of the beam increases durability and reduces overall construction cost. The yielding behavior of steel reinforcement provides ductility, whereas the FRP reinforcement contributes to load-carrying capacity [19].

In hybrid steel-FRP reinforced beams, FRP works as the main reinforcement, controlling the limit state, while steel determines the failure modes of such beams. Furthermore, steel reinforcement is placed deeper within the concrete, benefiting from a thicker protective concrete cover, which ensures ductile behavior of the beam [20].

Although concrete beams reinforced with hybrid steel-FRP beams provide some key advantages, the reinforcement configuration must be optimized to increase both strength and ductility. Their combined performance should guarantee the safe operation of the structure. In recent years, extensive research worldwide has been devoted to beams reinforced with hybrid steel-FRP bars. These studies have presented improved theoretical models and identified optimal reinforcement parameters [21].

METHODOLGY

Determining and analyzing the stresses generated in the rebar of reinforced concrete members is important for evaluating their load-bearing capacity, crack resistance, and overall response. Precise results on the internal stress state of reinforcement are essential for verifying theoretical assumptions, improving design techniques, and also ensuring compliance with safety and performance requirements. However, obtaining such data experimentally in full-scale or laboratory-tested specimens is associated with a number of significant challenges and limitations [5].

Measurement of stresses in rebar embedded in concrete member can be a difficult the use of highly specialized and sensitive equipment, including strain gauges, load cells, and various other precision sensors. The installation of these devices must be performed with high accuracy to ensure proper data acquisition, often demanding modifications to the reinforcement or concrete placement techniques. Moreover, it is nearly impossible to install measuring devices on every reinforcement bar, or even on a sufficient number of bars to produce a representative stress map. It is very challenging to place sensors at all important locations due to the confined nature of reinforced concrete members and the intricate interaction between reinforcement and surrounding concrete. This process becomes time-consuming, labor-intensive, and expensive even when it is possible [7, 12]. Because of this, it is frequently impossible or ineffective to measure stress thoroughly throughout a structural member's entire reinforcement layout (Figure 1).

Given these constraints, modern numerical simulation software can be an effective and powerful alternative for experimental tests. Finite element method based on software such as ANSYS provides the opportunity to make an accurate model the geometric characteristics of the reinforced concrete member, define the mechanical properties of both concrete and reinforcement considering nonlinear properties, and replicate real loading and boundary conditions with high precision. Utilizing these numerical models, it becomes possible to get detailed distributions of normal

stresses, shear stresses, strains, and other mechanical parameters within both the concrete and the reinforcement. Such modeling allows scholars to study structural behavior at any chosen time and any part of the member, which cannot be achieved even with advanced experimental instrumentation. The ability to perform parametric studies, such as changing reinforcement ratios, adjusting nonlinear material properties, makes numerical modeling much more effective. It gives researchers the opportunity to evaluate structural behavior in detail without having to build and test many physical specimens [13, 19].

A total of nine types of beams were selected for the numerical investigation. The cross-section of the specimens is rectangular, with a width of 150 mm and a height of 200 mm. The beams were tested under four-point bending to determine the normal stresses in both the steel and GFRP reinforcement, as well as in the concrete. The geometric parameters and reinforcement layout are shown in Figure 1.

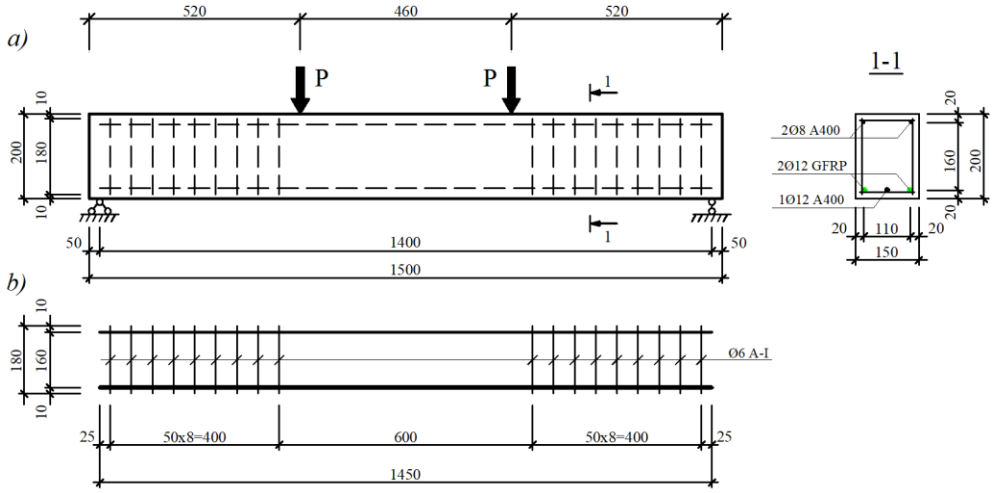

FIGURE 1. Beam geometry and reinforcement layout (the cross section of B3-1S12-2G12 is shown for reference): *a*) concrete beam; *b*) reinforcement layout;

Beams were divided into three groups depending on the reinforcement arrangement in the tension zone. In Group 1, three reinforcement bars were placed in one layer; in Group 2, four reinforcement bars were arranged in one layer; and in Group 3, five bars were placed in two layers with adequate spacing between them. All reinforcement diameters, quantities, cross-sectional areas, reinforcement ratios, and concrete strengths are shown in Table 1.

TABLE 1. Characteristics of reinforcements and concrete used for the beams

Beam notation	Tension steel rebar	Tension GFRP	Steel bar area A_s, cm^2	GFRP bar area A_f, cm^2	Ratio A_f / A_s	Steel reinforcement ratio μ_s, %	GFRP reinforcement ratio μ_f, %	Concrete strength, MPa
B1-3S12	3Ø12 A400	-	3.39	-	-	1,26		31,2
B2-1S12-2G10	1Ø12 A400	2Ø10	1.13	1.57	1.39	0,42	0,58	31,2
B3-1S12-2G12	1Ø12 A400	2Ø12	1.13	2.26	2	0,42	0,84	31,2
B4-4S12	4Ø12 A400	-	4.52	-	-	1,68		30,2
B5-2S12-2G12	2Ø12 A400	2Ø12	2.26	2.26	1	0,84	0,84	30,2
B6-2S10-2G12	2Ø10 A400	2Ø12	1.57	2.26	1.44	0,58	0,84	30,2
B7-5S10	5Ø10 A400	-	3.93	-	-	1,59		30,8
B8-3S10-2G10	3Ø10 A400	2Ø10	2.36	1.57	0.67	0,98	0,58	30,8
B9-2S10-3G10	2Ø10 A400	3Ø10	1.57	2.36	1.5	0,65	0,87	30,8

RESEARCH RESULTS

Table 2 presents the normal stresses developed in the longitudinal reinforcement located in the tension and compression zones of all beams, along with their ultimate load-carrying capacities and maximum deflection values.

The analysis shows that the average normal stresses in the steel reinforcement in the tension zone were between 450 and 505 MPa in the specimens, consistently exceeding the yield stress depending on reinforcement ratio of the beam. For example, B2-1S12-2G10 and B4-4S12 beams displayed tension steel stresses of 504.32 MPa and 442.41 MPa, respectively, that the steel rebar yielded and subsequently transitioned into the strain-hardening stage which helped prevent sudden failure of the beam. This behavior demonstrates that the beams were capable of carrying additional loads beyond initial yielding which gives more safety, showcasing the ductile performance of steel reinforcement in hybrid and traditional steel reinforced concrete beams.

TABLE 2. Normal stresses in the reinforcement located in the tension and compression zones of the beam

Beam notation	Ultimate load P_u, кН	Ultimate moment M_u, kN·m	Maximum deflection f, mm	Normal stress in tension steel rebar, MPa	Normal stress in GFRP rebar, MPa	Normal stress in compression rebar, MPa
B1-3S12	106.6	24.87	15.15	488.98		405.01
B2-1S12-2G10	100.2	23.38	21.36	504.32	623.28	404.23
B3-1S12-2G12	106.5	24.85	17.79	479.49	493.37	403.61
B4-4S12	129.1	30.12	9.01	442.41		418.23
B5-2S12-2G12	120.01	28.00	16.12	460.43	402.17	408.29
B6-2S10-2G12	110.7	25.83	15.9	469.09	440.05	403.54
B7-5S10	107.05	24.98	13.98	475.41		406.03
B8-3S10-2G10	105.7	24.66	18.73	477.31	488.99	409.70
B9-2S10-3G10	102.1	23.82	15.89	448.37	442.28	403.69

In the compression zones, the normal stresses in the reinforcement were also close to or above 400 MPa for all beams. Compression stresses ranged from approximately 403 MPa (B3-1S12-2G12) to 418 MPa (B4-4S12), therefore, the compression rebar reached its ultimate strength under loading. This presents that the compression bars were engaged in resisting applied loads and contributed slightly to the balanced stress distribution between the tension and compression zones. Notably, beams with higher reinforcement ratios, such as B4-4S12 (μ=1.68%), generated both higher load-bearing capacity (129.1 kN) and higher compression stress, demonstrating the direct influence of reinforcement content on overall beam performance (Figure 2).

The behavior of the GFRP reinforcement in the tension zone illustrated a wider stress range, changing from 402 MPa to over 620 MPa. The highest value 623.28 MPa was observed in beam B2-1S12-2G10, which had a relatively low steel reinforcement ratio (μ = 1.0%). This indicates that when a beam has less steel reinforcement ratio, the GFRP bars participate more significantly in receiving tensile forces. In contrast, beams have equal cross section areas of steel and GFRP reinforcements (e.g., B5-2S12-2G12) observed lower GFRP stresses (402.17 MPa). This means tensile forces distributed equally between GFRP and steel bars (Figure 2).

Deflection values also changed significantly from one beam to another, indicating how stiffness of the beams changed with different reinforcement ratio. For example, B1-3S12 and B2-1S12-2G10 had some of the largest deflections 15.15 mm and 21.36 mm which reflects their higher deformability under loading, especially in specimens with different reinforcement ratios. When the reinforcement ratio was the same in B1-3S12 and B3-1S12-2G12, the deflections were 15.15 mm and 17.79 mm, respectively. On the other hand, beams with more steel reinforcement such as B4-4S12, which had 4.524 cm² of steel showed much smaller deflections, only about 9.01 mm. This clearly presents adding more steel increases the beam's stiffness and reduces its deflection (Table 1).

Overall, the detailed analysis of Table 1 demonstrates that both steel and GFRP reinforcements effectively received the applied loads, even as stresses approached or reached ultimate values of material. The interaction between reinforcement type, reinforcement ratio, stress distribution, and deflection behavior shows that the selected reinforcement schemes were both technically and structurally efficient. The results highlight the benefits of using hybrid steel-GFRP reinforced concrete beams. This combination not only enhances the beams' strength and ductility but also makes material use more efficient and improves their overall load-carrying capacity.

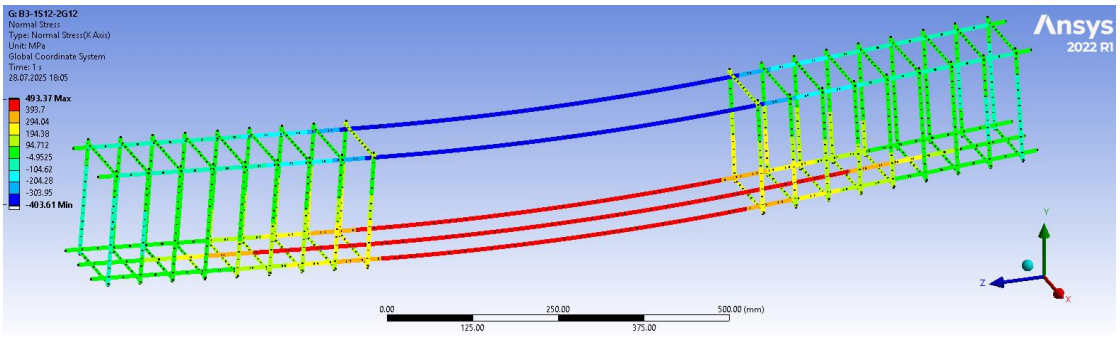

B3-1S12-2G12

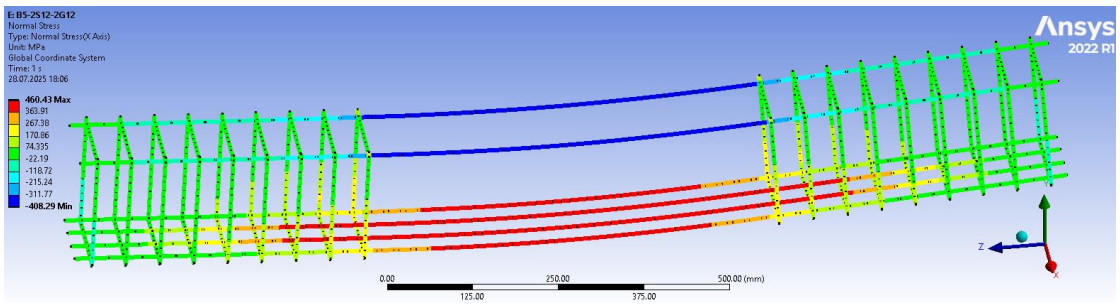

B5-2S12-2G12

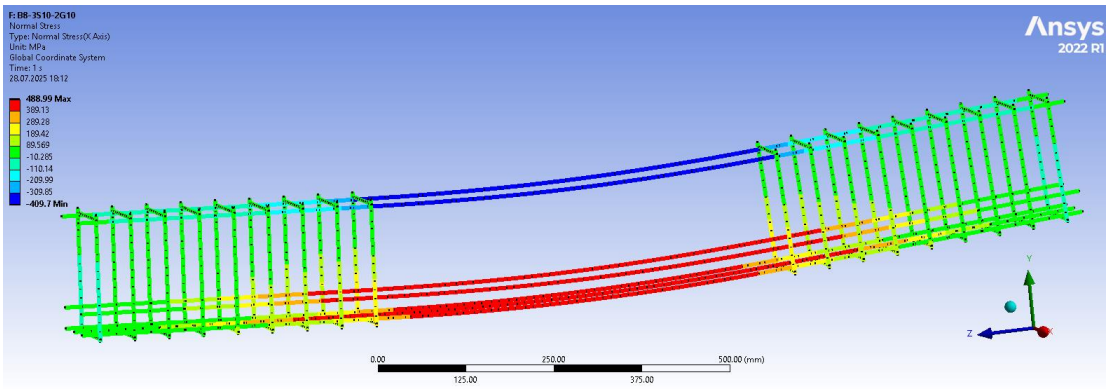

B8-3S10-2G10

FIGURE 2. Normal stresses in the reinforcements

The modeling results in Figure 3 show that the maximum compressive stress in the concrete was concentrated in the beam's compression zone, reaching 5.83 MPa at the point where the load was applied. This high stress level developed because the concrete entered a more intense state of compression under the centrally applied load. Since the load was applied at l/3 distance, the internal forces shifted toward the upper fibers of the section, causing the compressive stresses there to steadily increase as the load grew.

The nature and magnitude of such compressive stresses are directly associated with the inherent mechanical properties of the concrete including compressive strength, modulus of elasticity, and stress-strain behavior, and the characteristics of applied loading scheme. The current case successfully embodies the resistance of the concrete to the external loading as well as how the response of the deformation of the structure can be observed with the rising compressive demand by obtaining numerical outcomes. This action is aligned with the classical bending theory where the concrete within compression zone contributes significantly towards the bending of internal forces.

Furthermore, the results demonstrate that the compressive stresses developed in the upper zone of the beam approach the concrete's ultimate compressive strength. Achieving stress levels that are close to this limit is an important signifier that can be used to assess the performance of the beam in terms of its structure since it means that the section is approaching the limit state. This type of information is required to determine the strength capacity and

the deformation properties of the concrete, and to determine whether the structural design is sufficient in extreme loading.

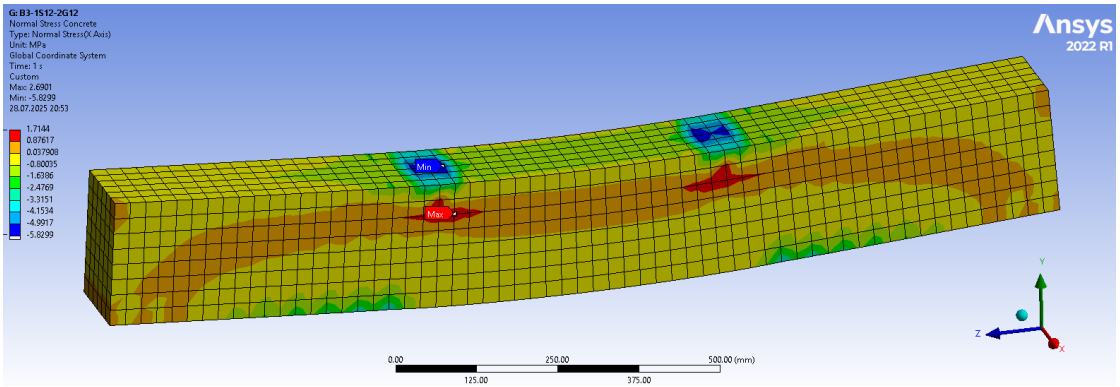

FIGURE 3. Normal stresses in the concrete of the B3-1S12-2G12 beam

The concrete strain is generally known to be one of the most important parameters in assessing the structural performance and deformation characteristics of the reinforced concrete members. The maximum strains that were generated in the compression and tension zones of the beam are noted in the regions of blue and red respectively as shown in Figure 4. At the compression zone, the concrete reached its maximum compressive strain, $\varepsilon_{b1,red}=0.0015$, that was equivalent to the occurrence of local failure. This observation highlights that concrete has a very limited capacity to deform when compressive stress is high and it is critical to carefully model strain distributions in in numerical analysis. The highest relative strain occurred at the tension zone where $\varepsilon_{bt}=0.00062$ was recorded which indicates the response of the concrete to the tensile forces being passed through the reinforcements. Monitoring of these strain levels is valuable in terms of the interaction of concrete and reinforcement, especially how the beam can sustain loads beyond the elastic range, and it can be better used to evaluate the ductility and the overall structural behavior of the material.

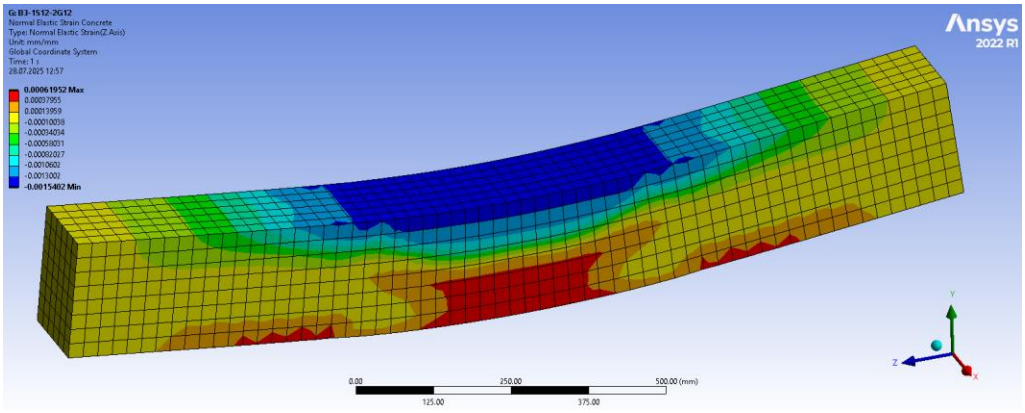

FIGURE 4. Strains in the B3-1S12-2G12 beam

The results of the ANSYS software in the numerical modeling of beams indicate that there is a considerable difference in the cracking behavior of conventional reinforced concrete beams and hybrid steel GFRP reinforced concrete beams. The onset of cracks was noted in the conventional steel reinforced concrete beams at a rather advanced stage of loading, specifically when the load applied was about 14-15% of the ultimate load bearing capacity. This delayed crack formation is a reflection that the steel reinforcement is actually operating to resist tensile action during the initial loading period, and thus slowing down the initiation of visible cracking (table 3).

In contrast, the hybrid steel-GFRP reinforced concrete beams showed the first cracking at a slightly lower load which is about 11-13 % of the ultimate load capacity. The main reason one can state why this cracking has been experienced earlier in hybrid reinforced concrete beams is the fact that the modulus of elasticity of the FRP reinforcement is relatively lower when compared to steel. The lower stiffness of the GFRP brings a slight change in

the stress distribution within the tension zone resulting in the earlier tensile strain accumulation the concrete and therefore the earlier crack formation.

TABLE 3. Cracking moment for beam specimens

Beam notation	M_{crc}^{num}, kN·m	M_{u}^{num}, kN·m	$M_{crc}^{num} / M_{u}^{num}$
B1-3S12	3.73	24.87	0.15
B2-1S12-2G10	3.04	23.38	0.13
B3-1S12-2G12	3.23	24.85	0.13
B4-4S12	4.22	30.12	0.14
B5-2S12-2G12	3.08	28.00	0.11
B6-2S10-2G12	3.10	25.83	0.12
B7-5S10	3.75	24.98	0.15
B8-3S10-2G10	3.21	24.66	0.13
B9-2S10-3G10	3.10	23.82	0.13

Table 3 gives a detailed overview of the moments of crack initiation of all beam specimens, and the difference in the loads at which the initial cracks are formed are clearly visible. These observations emphasize the important role of the type of reinforcement on the early-stage of structural performance of reinforced concrete beams. Notably, the hybrid reinforcement can cause the earlier crack initiation, however, this does not necessarily reduce the total load-carrying capacity of the beams. The GFRP reinforcement continues to contribute effectively to the post-cracking behavior and the ductility of the beams as well as providing the beams the ability to withstand additional loading beyond the initial cracking stage. Therefore, the relationship between steel and FRP reinforcement in hybrid reinforcement requires that the relationship be known to predict properly cracking behavior, serviceability performance, and design of ductile reinforced concrete element when subjected to applied loads.

CONCLUSIONS

According to the numerical investigation, both steel and GFRP bars contribute positively to the concrete beams behavior. Steel in the tension zone exceeded the yield stress, which allowed it remain ductile and provided extra safety after yielding. Depending on the ratio relative to steel, GFRP bars received a significant part of tensile forces, with stress values ranging from moderate to high, particularly in beams with lower amount of steel. The compression rebar also contributed slightly to resisting loads and distributed stresses along the section. A balanced combination of crack resistance and load-carrying capacity was observed in hybrid steel-GFRP reinforced concrete beams. Cracks start earlier in hybrid beams due to the lower stiffness of GFRP bars, their overall load-carrying capacity is not significantly lower than conventional reinforced concrete beams. Steel reinforcements in hybrid steel-GFRP reinforced concrete beams provide ductility and control deflections, at the same time GFRP bars increase tensile strength and contribute better performance once cracking occurs. The concrete stresses in the compression zone reached its ultimate values, which establishes its active participation in resisting applied loads. Overall, hybrid steel-GFRP rebar is an important and practical solution for the exploitation of beams under applied load. Moreover, it increases durability, safety, and cost-effectiveness compared to conventional steel reinforced concrete beams.

REFERENCES

1. Ruan X., Lu C., Xu K., Xuan G., Ni M., Flexural behavior and serviceability of concrete beams hybrid-reinforced with GFRP bars and steel bars // Composite Structures – 2019. https://doi.org/10.1016/j.compstruct.2019.111772
2. Dang V.H., Nguyen P.D. Experimental and Theoretical Analysis of Cracking Moment of Concrete Beams Reinforced with Hybrid Fiber Reinforced Polymer and Steel Rebars // Advances in Technology Innovation, Vol. 6, No. 4, 2021, p. 222-234. https://doi.org/10.46604/aiti.2021.7330
3. Ge W., Ashour A.F., Yu J., Gao P., Cao D., Cai C., and Ji X. Flexural Behavior of ECC–Concrete Hybrid Composite Beams Reinforced with FRP and Steel Bars // Journal of Composites for Construction, ISSN 1090-0268 – 2018. https://doi.org/10.1061/(ASCE)CC.1943-5614.0000910
4. Abduljabbar M.S., Abdulsahib W.S. Flexural Performance of Concrete Beams Reinforced with Hybrid FRP-Steel Bars: A mini review // Engineering and Technology Journal 41 (05) (2023) 619- 628. http://doi.org/10.30684/etj.2022.135764.1284

5. Ravshanbek Mavlonov, and Sobirjon Razzakov. Numerical modeling of combined reinforcement concrete beam. E3S Web of Conferences 401, 03007 (2023) CONMECHYDRO – 2023. https://doi.org/10.1051/e3sconf/202340103007
6. Barris, C., Torres L., Turon A., Baena M., Mias C. An experimental study of the flexural behaviour of GFRP RC beams and comparison with prediction models // Composite Structures Volume 91, Issue 3, December 2009, p. 286-295. https://doi.org/10.1016/j.compstruct.2009.05.005
7. Hemalatha K., Ravi Prasad D. Numerical analysis on reinforcement ratio of RC beams using FRP and steel rebars // E3S Web of Conferences 391, 01210 (2023), ICMED-ICMPC 2023. https://doi.org/10.1051/e3sconf/202339101210
8. Alkhudery H., Albuthbahak O., and Alkatib H. Investigation of Effective Hybrid FRP and Steel Reinforcement Ratio for Concrete Members // Journal of Engineering and Applied Sciences, vol. 13, no. 13, pp. 5150-5161, September 2018. http://dx.doi.org/10.3923/jeasci.2018.5150.5161
9. Renyuan Q, Zhou A, Lau D, Effect of reinforcement ratio on the flexural performance of hybrid FRP reinforced concrete beams // Composites Part B: Engineering, Volume 108, 1 January 2017, p. 200-209. https://doi.org/10.1016/j.compositesb.2016.09.054
10. Nguyen T.h., Nguyen V.T. and Phan M.T. Experimental study on the flexural behaviour of corroded concrete beams reinforced with hybrid steel/GFRP bars // Structure and Infrastructure Engineering, Volume 20, 2024 - Issue 6. https://doi.org/10.1080/15732479.2022.2123530
11. Araba A.M., Ashour A.F. Flexural performance of hybrid GFRP-Steel reinforced concrete continuous beams // Composites Part B (2018), https://doi:10.1016/j.compositesb.2018.08.077
12. Ravshanbek Mavlonov, Sobirjon Razzakov, and Sohiba Numanova. Stress-strain state of combined steel-FRP reinforced concrete beams. E3S Web of Conferences 452, 06022 (2023) IPFA 2023, https://doi.org/10.1051/e3sconf/202345206022
13. Bencardino F., Condello A., Ombres L. Numerical and analytical modeling of concrete beams with steel, FRP and hybrid FRP-steel reinforcements // Composite Structures 140 – 2016, p. 53–65. http://dx.doi.org/10.1016/j.compstruct.2015.12.045
14. Devaraj R., Olofinjana A., Gerber C. Making a Case for Hybrid GFRP-Steel Reinforcement System in Concrete Beams: An Overview. Applied Sciences, MDPI. 2023, 13, 1463. https://doi.org/10.3390/app13031463
15. A. Martazaev and S. Khakimov, "Dispersed reinforcement with basalt fibers and strength of fiber-reinforced concrete beams," AIP Conf. Proc. 3256, 030011 (2025). https://doi.org/10.1063/5.0266797
16. Bingyan Wei, Xiongjun He, Ming Zhou, Huayi Wang, Jia He. Experimental study on flexural behaviors of FRP and steel bars hybrid reinforced concrete beams. Case Studies in Construction Materials 20 (2024) e02759, https://doi.org/10.1016/j.cscm.2023.e02759
17. S. Razzakov and A. Martazaev, Mechanical properties of concrete reinforced with basalt fibers, E3S Web Conf. 401, 05003 (2023); https://doi.org/10.1051/e3sconf/202340105003
18. Elgabbas F., Ahmed E.A., and Benmokrane B. Flexural Behavior of Concrete Beams Reinforced with Ribbed Basalt-FRP Bars under Static Loads // Journal of Composites for Construction. Vol. 21, No. 3. https://doi.org/10.1061/(ASCE)CC.1943-5614.0000752
19. Hawileh, R., Finite element modeling of reinforced concrete beams with a hybrid combination of steel and aramid reinforcement // Materials and Design – 2014. http://dx.doi.org/10.1016/j.matdes.2014.10.004
20. A. Martazaev, M. Orzimatova, and M. Xamdamova, "Determination of optimum quantity of silica fume for high-performance concrete," AIP Conf. Proc. 3256, 030012 (2025). https://doi.org/10.1063/5.0266799
21. Xingyu G., Yiqing D., Jiwang J. Flexural behavior investigation of steel-GFRP hybrid-reinforced concrete beams based on experimental and numerical methods // Engineering Structures Volume 206, 1 March 2020, 110117. https://doi.org/10.1016/j.engstruct.2019.110117
22. Pang L., Qu W., Zhu P. and Xu J. Design Propositions for Hybrid FRP-Steel Reinforced Concrete Beams // Journal of Composites for Construction – 2015, © ASCE, ISSN 1090-0268. http://dx.doi.org/10.1061/(ASCE)CC.1943-5614.0000654